THE ASTROPHYSICAL JOURNAL, 457:L81–L84, 1996 February 1

GIANT RADIO PULSES FROM A MILLISECOND PULSAR

I. COGNARD,[1] J. A. SHRAUNER,[2] J. H. TAYLOR,[3] AND S. E. THORSETT[4]
Joseph Henry Laboratories and Physics Department, Princeton University, Princeton, NJ 08544
Received 1995 July 11; accepted 1995 November 21

ABSTRACT

We have observed 1.7×10^6 individual pulses from the millisecond pulsar PSR B1937+21. About one pulse in 10,000 has more than 20 times the mean "pulse-on" flux density, and individual pulses as large as 300 times the average were observed. Comparable behavior has previously been observed only for the Crab pulsar. Giant pulses from PSR B1937+21 are seen in both the main pulse and interpulse components, and their amplitude distribution has roughly a power-law shape. Strong pulses differ greatly from the average emission: they are narrower, systematically delayed by some 40–50 μs, and many are nearly 100% circularly polarized. In addition to their potential importance for elucidating the physics of the emission region, the giant pulses may be useful for high precision timing measurements.

Subject headings: pulsars — pulsars: individual (PSR B1937+21)

1. INTRODUCTION

The Crab pulsar (PSR B0531+21) and the millisecond pulsar PSR B1937+21 are both remarkable, but for different reasons. The Crab is the youngest known pulsar, born in A.D. 1054, whereas PSR B1937+21 is among the older ones, with a spin-down timescale of 2×10^8 yr. The 4×10^{12} G magnetic field of the Crab pulsar is 10^4 times stronger than that of PSR B1937+21, and although the Crab is the fastest of the high-field ($B \gtrsim 10^{11}$ G) pulsars, with a period $P = 33$ ms, it is 20 times slower than the 1.56 ms PSR B1937+21.

Given their differences, it is perhaps surprising that these two pulsars are the only ones known occasionally to produce radio pulses hundreds of times brighter than a typical pulse. In the Crab these have been called "giant" pulses, and they have been observed and studied since the pulsar was discovered (Staelin & Reifenstein 1968; Staelin & Sutton 1970; Heiles, Campbell, & Rankin 1970; Gower & Argyle 1972; Lundgren 1994; Lundgren et al. 1995). In contrast, the existence of large pulses from PSR B1937+21, first noted by Wolszczan, Cordes, & Stinebring (1984), has received little attention—in part because the fast pulsar period, large dispersive smearing timescale, and relatively weak signal conspire to make single-pulse observations difficult. Recently, observations by Sallmen & Backer (1995; see also Backer 1995) have confirmed the observations of Wolszczan et al. and have emphasized the peculiarity of the strong pulses, but their results were limited by the small number of pulses observed. Whereas studies of the Crab pulsar have used over 100 hr of data (Lundgren 1994), Sallmen & Backer present analysis of only 16,800 pulse periods, or 26 s.

New data recording and computer technologies have simplified the implementation of digital techniques for the coherent removal of interstellar dispersion from pulsar signals. While testing a new observing system briefly described in § 2, we collected and studied 44 minutes of data from PSR B1937+21 with 1.2 μs time resolution. We have confirmed the existence of giant radio pulses from this pulsar; in § 3 we describe their temporal properties and distribution of intensities. In § 4 we discuss some questions raised for studies of the pulsar emission mechanism, and we call attention to the importance of giant pulse observations for pulsar timing measurements.

2. OBSERVATIONS AND SIGNAL PROCESSING

Our observations were made with the 305 m Arecibo telescope on 1994 November 26. Two orthogonal, circularly polarized signals were received at 430 MHz, converted to 30 MHz, passed through 500 kHz Gaussian-shaped bandpass filters, and mixed to base band with a pair of local oscillators in phase quadrature. Real and imaginary parts of the resulting complex signals were 2-bit sampled every 1.2 μs, packed into bytes, and written in alternating blocks to a pair of Exabyte magnetic tape drives. Some 44 minutes of continuous data were collected, comprising 1,695,542 pulse periods.

Dispersion in the ionized interstellar medium produces a 3.7 ms differential delay across our 500 kHz bandpass. This delay is more than twice the pulsar period, so it would completely smear out the pulsed signal if not removed. We eliminated the dispersion by using the coherent signal-processing technique described by Hankins & Rickett (1975), effectively convolving the signal with a complex chirp function designed to cancel the progressive phase retardation as a function of frequency caused by the interstellar medium. Signals from the two polarizations were then squared and cross-multiplied to produce the four Stokes parameters of the received signal. Polarization data were calibrated by normalizing the off-pulse noise levels in each digitized channel, and the effect of parallactic angle rotation during the 44 minutes observation was removed. We did not attempt to correct for cross-coupling between the nominally orthogonal circular feeds; we believe that resulting errors in the inferred circular polarization should amount to no more than a few percent (see Rankin, Cambell, & Spangler 1975).

The corrected Stokes parameters were folded synchronously with the known topocentric pulsar period to produce an average profile including full polarization information. The results, shown in Figure 1, are in excellent agreement with previous observations at this frequency (Thorsett & Stinebring

[1] E-mail: ismael@pulsar.princeton.edu.
[2] E-mail: jay@pulsar.princeton.edu.
[3] E-mail: joe@pulsar.princeton.edu.
[4] E-mail: steve@pulsar.princeton.edu.

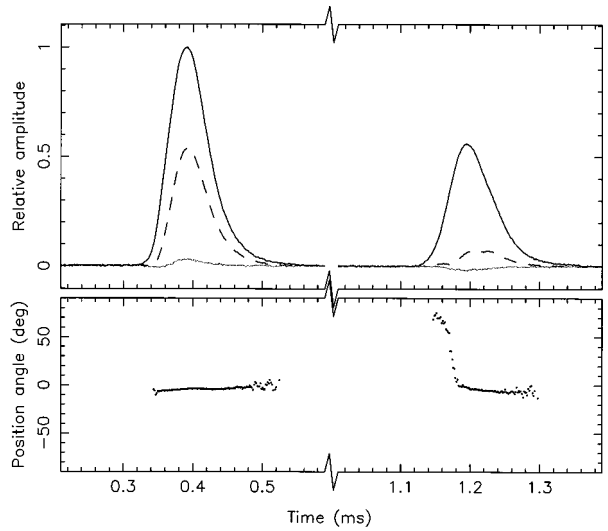

FIG. 1.—Average profile of PSR B1937+21, comprised of 1.7×10^6 individual pulses (about 44 minutes of data), plotted with 1.5 μs resolution. The solid line represents total intensity, while the dashed and gray lines give the linear and circular polarization components, respectively. The polarization position angle (measured counterclockwise on the sky, with arbitrary origin) is shown in the lower panel.

1990). The PSR B1937+21 main pulse (MP) is more than 50% linearly polarized, with little if any circular polarization; the interpulse (IP) peaks at about 13% polarization near its center, with perhaps a few percent of circular polarization as well. The position angles change only slightly over most of the polarized zones.

3. GIANT PULSES FROM PSR B1937+21

In order to search for giant radio pulses, we computed the total flux in rectangular windows centered on the MP and IP. The strongest pulses found in each window are illustrated in the top panel of Figure 2. Because the real and imaginary parts of the predetection signals in each circular polarization have Gaussian amplitude distributions with equal variance, the unsmoothed intensity estimates have χ^2 distributions with 4 degrees of freedom. The rms intensity deviation is therefore 71% of the mean, and this fully accounts for the deep modulation and apparent pulse structure observed. It is unlikely that we are observing the intrinsic fine structure of the signal because multipath scattering in the interstellar medium will largely mask any such effects at our relatively low observing frequency. The scattering timescale to $1/e$ intensity was found to be 25 ± 5 μs, in agreement with previous measurements (Cordes et al. 1990).

All strong individual pulses that we detected were located on the trailing edges of the MP or IP, a behavior noted also by Backer (1995). To improve our sensitivity to giant pulses, we repeated the search by including only the trailing wings of the pulse and interpulse in the trigger windows. However, the windows were kept wide enough to include all of the observed giant-pulse emission from the first pass. For each pulse period we calculate the ratios S_m and S_i of mean flux density to the average in the defined MP and IP windows. The cumulative probability distributions of S_m and S_i are shown in Figure 3. Since the average signal-to-noise ratio per pulse is about 0.5 in the MP and 0.3 in the IP, the observed distributions are dominated at low intensities by Gaussian background noise.

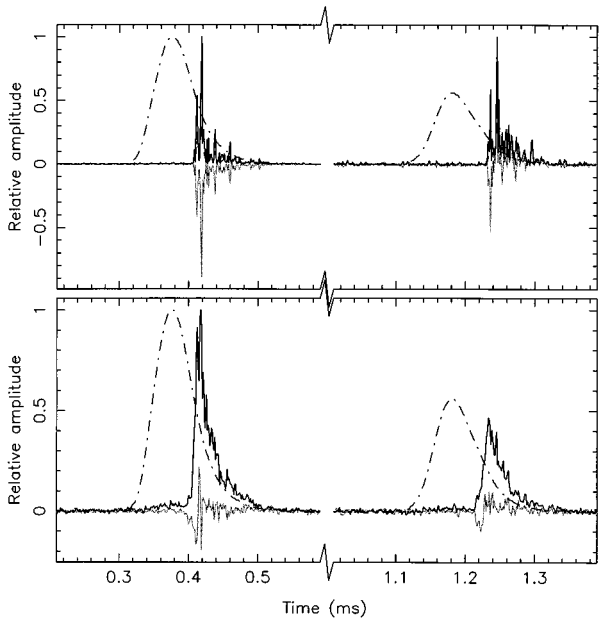

FIG. 2.—*Top*: Strongest single pulses in the main pulse and interpulse. The noise is $\chi^2(4)$ distributed, which accounts for the deep modulation. *Middle and bottom*: Average shapes of the 60 strongest pulses in the MP and IP regions. Circular polarization is indicated as in Fig. 1; linear polarization (not shown) was no more than a few percent. Dot-dashed lines represent the time-aligned average of all 1.7×10^6 pulses. The data are displayed at full 1.2 μs resolution; main pulses of the averages, and the two individual pulses in the top panel, have been separately normalized to unity.

However, for amplitudes well above the noise, both the MP and IP show essentially power-law distributions. Moreover, the MP and IP amplitude distributions have consistent power-law indices and frequency-of-occurrence levels. Thus, if the giant pulses are normalized to the local mean flux density, it appears we can describe them with a single probability distribution. If f is the fraction of pulses or interpulses stronger than S times the mean, then for $S \gtrsim 15$ we find that

$$f = f_0 S^{\alpha}, \tag{1}$$

with $f_0 = 0.032 \pm 0.008$ and $\alpha = -1.8 \pm 0.1$. This relation is illustrated by the sloping straight line plotted in Figure 3.

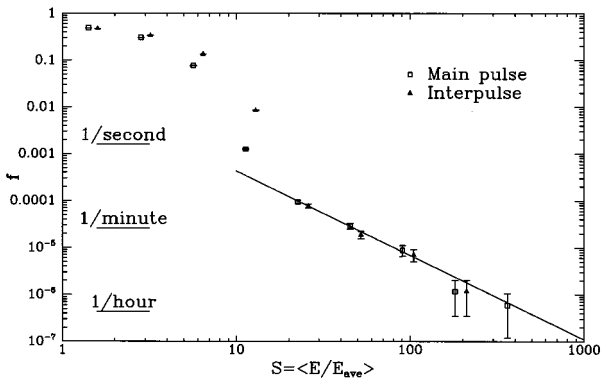

FIG. 3.—Cumulative distribution of pulse amplitudes greater than S, measured in units of the mean amplitudes in the main pulse and interpulse windows. (The means are approximately 1.5 Jy and 0.8 Jy, respectively.) For amplitudes $S \lesssim 11$ for the main pulse and $S \lesssim 20$ for the interpulse, the distributions are dominated by background noise. The solid line is a power-law fit of eq. (1) to the rightmost nine data points.

Although the average of 60 giant pulses shows only slight polarization (Fig. 2), many individual giant pulses exhibit strong circular polarization. For example, the strongest pulse observed (Fig. 2, *top left*) is over 90% left-circularly polarized. Giant pulses with both signs and high fractions of circular polarization are observed, with high statistical significance. Such emission is unusual among astronomical sources.

4. DISCUSSION

Single-pulse studies have been carried out for a few dozen of the strongest pulsars (see, for example, Hesse & Wielebinski 1974; Taylor, Manchester, & Huguenin 1975; Ritchings 1976). Histograms of single-pulse intensities have been shown to have approximately one-sided exponential shapes, with maxima somewhere between zero and the mean and high-amplitude tails out to 4–10 times the mean. With the exception of the Crab pulsar and PSR B1937+21, pulses much stronger than 10 times the mean have not been observed, even rarely. A highly sensitive search for isolated dispersed pulses was carried out some years ago by Phinney & Taylor (1979), using the pulsar survey data of Hulse & Taylor (1975; see also Hulse 1975). This search would have been very sensitive to pulsars with occasional giant pulses, even if their mean flux densities were well below the Hulse & Taylor (1975) survey limit. No such strongly modulated pulsars were found; it is clear that pulsars with giant pulses are quite uncommon.

On the other hand, the Crab pulsar was first detected in just such a search for strong individual pulses (Staelin & Reifenstein 1968). This pulsar has long been known to have an extended high-amplitude tail in its distribution of pulse intensities, extending out to at least several hundred times the mean (Argyle & Gower 1972; Gower & Argyle 1972; Lundgren 1994; Lundgren et al. 1995). Fitting equation (1) to the distribution of giant-pulse amplitudes gives $\alpha = -2.5$ for the Crab at 146 MHz (Argyle & Gower 1972) and -2.46 ± 0.04 at 812 MHz (Lundgren 1994). [The apparent discrepancy in the value of α noted by Lundgren seems to arise from an inconsistent definition of $f(S)$.] For the Crab pulsar the amplitude distribution is considerably steeper in the interpulse, with $\alpha = -2.8$ (Argyle & Gower 1972). Because of the difference in power-law slopes, as well as differences in the way peak-to-mean flux ratios are calculated and possible difference in the relative spectra of giant pulses and normal emission, it is less meaningful to compare the frequencies of occurrence of giant pulses for the two pulsars. However, very roughly, we note that PSR B1937+21 exhibits a pulse or interpulse at least 100 times the mean signal level every 2 minutes, while the corresponding figure for the Crab (at 146 MHz) is about 3 hr (Argyle & Gower 1972). Expressed in pulsar periods, the corresponding time intervals are much more similar: approximately 0.8×10^5 and 3×10^5, respectively.

We consider it significant that the amplitude distributions of giant pulses from the pulse and interpulse of PSR B1937+21 agree not only in power-law index but also in fractional rate of occurrence. In the region of pulse phase where giant pulses are found, the average main pulse flux density is 1.8 times that of the interpulse; the average giant main pulse is also 1.8 times the average giant interpulse (see Fig. 3), which suggests that the same physical processes set the amplitude scales for both normal and giant pulses.

In both the MP and IP regions the giant-pulse emission is delayed relative to the average emission, as noted also by Backer (1995). We do not observe the phase jitter reported by Wolszczan et al. (1984); average polarized profiles of the 60 strongest pulses in each region are shown in the bottom two panels of Figure 2, and except for the larger estimation errors, every one of the single giant pulses looks very similar to their average, in both shape and alignment. The offset between peaks of the integrated profile and the average giant pulse is 38 ± 4 μs for the MP and 52 ± 4 μs for the IP. The giant-pulse and interpulse emission are thus separated by $189° \pm 1°$ of pulse longitude, as compared with 186° for the normal emission. At 1.4 GHz, high-resolution profiles of PSR B1937+21 show a notch on the trailing side of the MP and a less pronounced bump near the end of the IP. The separations of these features from the MP and IP maxima is similar to the giant-pulse offsets, and it seems very likely that this structure in the integrated profiles arises from the giant-pulse emission. At 430 MHz, the corresponding effect would be completely masked by the 25 μs broadening caused by interstellar scattering.

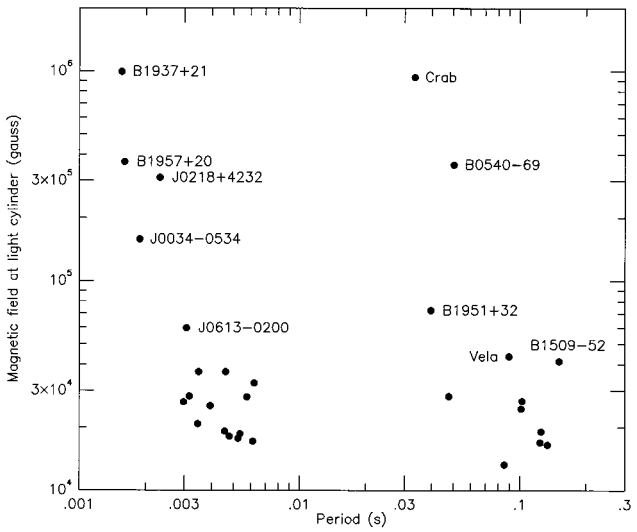

FIG. 4.—Among all known pulsars, the Crab and PSR B1937+21 have the largest estimated magnetic field strengths at the velocity-of-light cylinder. The top 30 such values for field pulsars are plotted here as a function of period.

In addition to the delay observed between the average emission and the giant pulses, one can see in Figure 2 that the rise time of the average shape of giant pulses is very short, not more than about 5 μs, or several of our nearly independent 1.2 μs samples. This fact reemphasizes that each giant pulse has a sharp rising edge at essentially the same arrival phase. Together with their high signal-to-noise ratios, the short rise time of the giant pulses could provide high-accuracy timing measurements based wholly on these pulses. Submicrosecond accuracy could probably be obtained, but further observations are needed to test the long-term stability of giant-pulse arrival.

Given the period and the period derivative of a pulsar, we can estimate the strength of the magnetic field at the light cylinder (where corotation would occur at the speed of light). With a conventional value for the polar field at the surface of the star and assuming a r^{-3} dependence, we calculate that the magnetic field strength at the light cylinder is $B_{lc} \sim 3 \times 10^8 \dot{P}^{1/2} P^{-5/2}$ G. Figure 4 shows the top 30 values obtained for all field pulsars, plotted as a function of period. (Pulsars in globular clusters were excluded because their period derivatives can be perturbed by gravitational interactions.) The two

largest values are for the Crab and PSR B1937+21, so it is interesting that these two pulsars are the only ones known to produce giant pulses. If the observed correlation is meaningful, it suggests that the giant-pulse emission physics may depend on conditions at the light cylinder, rather than close to the stellar surface. The strong circular polarization observed in individual pulses is an important constraint on the emission mechanism and region.

Our work probably raises more questions than it answers, and several additional investigations must be pursued. Simultaneous multifrequency observations would probe the instantaneous and average spectral properties of the giant pulses; timing measurements would test stability of the giant-pulse emission region; and extended observations with even a relatively small radio telescope could extend our knowledge of the giant-pulse distribution for PSR B1937+21 at high flux levels. Studies of young pulsars and other millisecond pulsars are also needed to test the hypothesis that strong magnetic fields at the light cylinder are a critical condition for giant-pulse activity. For a quarter century, giant radio pulses from the Crab have been treated as a unique phenomenon. The discovery of similar behavior in a millisecond pulsar emphasizes the importance of accounting for these pulses in any successful theory of the pulsar emission mechanism.

The Arecibo Observatory is operated by Cornell University under a Cooperative Agreement with the US National Science Foundation. We thank P. Perillat for extensive help with the observations and F. Camilo, R. Dewey, and D. Stinebring for helpful discussions. I. C. acknowledges support in part from a Lavoisier fellowship (Ministère des Affaires Etrangères, France) and from a Post-Doctoral fellowship (Conseil Régional du Centre, France).

REFERENCES

Argyle, E., & Gower, J. F. R. 1972, ApJ, 175, L89
Backer, D. C. 1995, Raman Research Institute Symp. on Pulsars, preprint
Cordes, J. M., Wolszczan, A., Dewey, R. J., Blaskiewicz, M., & Stinebring, D. R. 1990, ApJ, 349, 245
Gower, J. F. R., & Argyle, E. 1972, ApJ, 171, L23
Hankins, T. H., & Rickett, B. J. 1975, Meth. Comp. Phys., 14, 55
Heiles, C., Campbell, D. B., & Rankin, J. M. 1970, Nature, 226, 529
Hesse, K. H., & Wielebinski, R. 1974, A&A, 31, 409
Hulse, R. A. 1975, Ph.D. thesis, Univ. of Massachusetts
Hulse, R. A., & Taylor, J. H. 1975, ApJ, 201, L55
Lundgren, S. C. 1994, Ph.D. thesis, Cornell Univ.
Lundgren, S. C., Cordes, J. M., Ulmer, M., Matz, S. M., Lomatch, S., Foster, R. S., & Hankins, T. 1995, ApJ, 453, 433
Phinney, S., & Taylor, J. H. 1979, Nature, 277, 177
Rankin, J. M., Cambell, D. B., & Spangler, S. R. 1975, NAIC Rept. 46
Ritchings, R. T. 1976, MNRAS, 176, 249
Sallmen, S., & Backer, D. C. 1995, in ASP Conf. Proc. 72, Millisecond Pulsars: A Decade of Surprise, ed. A. S. Fruchter, M. Tavani, & D. C. Backer (San Francisco: ASP), 340
Staelin, D. H., & Reifenstein, E. C., III. 1968, Science, 162, 1481
Staelin, D. H., & Sutton, J. M. 1970, Nature, 226, 69
Taylor, J. H., Manchester, R. N., & Huguenin, G. R. 1975, ApJ, 195, 513
Thorsett, S. E., & Stinebring, D. R. 1990, ApJ, 361, 644
Wolszczan, A., Cordes, J. M., & Stinebring, D. R. 1984, in Millisecond Pulsars, ed. S. P. Reynolds & D. R. Stinebring (Green Bank: NRAO), 63